IEEE Access
Multidisciplinary | Rapid Review | Open Access Journal

Received 5 April 2023, accepted 27 April 2023, date of publication 4 May 2023, date of current version 17 May 2023.

Digital Object Identifier 10.1109/ACCESS.2023.3272898

RESEARCH ARTICLE

Design Optimization and Resonance Analysis of Rectangular Structured Moving Magnet Linear Actuator

MUHAMMAD JAWAD[1], HAITAO YU[1], ZAHOOR AHMAD[2], BASHARAT ULLAH[2], (Member, IEEE), AND BAHEEJ ALGHAMDI[3,4]

[1]School of Electrical Engineering, Southeast University, Nanjing 210096, China
[2]Department of Electrical and Computer Engineering, COMSATS University Islamabad, Abbottabad Campus, Abbottabad 22060, Pakistan
[3]Smart Grids Research Group, Center of Research Excellence in Renewable Energy and Power Systems, King Abdulaziz University, Jeddah 21589, Saudi Arabia
[4]Department of Electrical and Computer Engineering, Faculty of Engineering, King Abdulaziz University, Jeddah 21589, Saudi Arabia

Corresponding author: Haitao Yu (htyu@seu.edu.cn)

This work was supported in part by the Institutional Fund Projects under Grant IFPIP: 894-135-1443, and in part by the Ministry of Education and King Abdulaziz University, DSR, Jeddah, Saudi Arabia.

ABSTRACT This article examines a new linear oscillating actuator (LOA) design that uses rectangular-shaped core materials and permanent magnets (PMs). The primary objective of the paper is to examine a novel LOA topology with a rectangular-shaped core and PMs as an alternative to the tubular LOA. A static core material is housed between the mover's components and two stator cores with two coils, each of which is placed on either side of the mover. The dimensions of all the parameters are swept for optimization and the optimal parameter dimension is chosen based on the optimal value of the electromagnetic (EM) force. An analysis is done for output results like EM force and stroke. Parameters like input current, EM force and stroke-to-current ratio are investigated for different frequencies of the input electrical loading to demonstrate the significance of resonance operation. EM force per PM mass of the investigated design of LOA is 67 percent higher than that of a conventional rectangular-shaped LOA. Additionally, the EM force density of the proposed design is 23.8 percent higher than that of the conventional design of LOA. Furthermore, the stroke of the proposed LOA is also feasible and more than most of the designs of the LOA. Additionally, the proposed design of the LOA is simple in structure, low-cost, and feasible for fabrication.

INDEX TERMS Electromagnetic force, linear actuator, linear oscillatory force, moving magnet, rectangular topology.

I. INTRODUCTION

Linear actuators produce linear oscillatory EM forces within a specific range of oscillation amplitude (stroke) by using the electromagnetic actuation concept [1]. Traditionally, rotary motors were used to create linear oscillation by using crankshafts to transform electromagnetic torque into linear oscillatory EM force. The main issues with the crankshaft mechanism are more mechanical parts, more friction spots, and the use of the radial and tangential components of the force. Additionally, lubrication oil is essential for the crankshaft's long-term operation owing to that it has more friction points. Also, because of the more friction and the use of force components, the efficiency of the system degraded. On the contrary, LOA provides high-efficiency linear oscillatory EM force without using a crankshaft mechanism [2], [3].

The stator generates a controlled magnetic field, and the mover adjust its position in a way that the magnetic flux lines encounter the least reluctance [4]. Mover, the moving portion of the LOA oscillates on the same axis at a frequency equal to that of the input alternating electrical loading frequency. The operating frequency of the LOA is generally resonance frequency which is determined using the value of the mover mass and spring stiffness, attached to the mover. Reducing the mass of the mover is challenging, however it can be optimized to a certain value [5], [6].

The associate editor coordinating the review of this manuscript and approving it for publication was Qinfen Lu.

This work is licensed under a Creative Commons Attribution-NonCommercial-NoDerivatives 4.0 License.
For more information, see https://creativecommons.org/licenses/by-nc-nd/4.0/

In the literature, there are three basic types of LOA based on the components placed on the mover: moving coil, moving iron, and moving magnet [7], [8], [9]. Moving coil performs better in terms of cost, but challenging during the electrical loading of the moving part. Additionally, moving coil LOA performs poorly in EM force compared to moving magnet LOA. Due to the lack of an active part on its mover, moving iron LOA is more advantageous in terms of cost. The primary consequence of the moving iron LOA is high mover mass. On the other hand, moving magnet LOA provides high EM flux density, better EM force, and high efficiency. Additionally, the moving magnet LOA mover mass is low, due to which the resonance frequency value is high, resulting in high output power and mass flow rate [5].

Two types of LOA design structures, rectangular and tubular, are made to produce linear oscillatory EM force. Tubular topology has high air gap flux density and EM force density due to its compactness. The end winding effect is also absent in LOA that has a tubular-shaped topology [10]. The limitation of the tubular structure is complex lamination fabrication for lowering the core losses. Additionally, moving magnet LOA with a tubular structure has tubular-shaped PMs, which are expensive due to their complicated manufacturing. Combining several arc-shaped PMs to achieve radial magnetization of tubular PMs results in a less-than-perfect magnetization pattern and reduced mechanical strength of the mover [11]. Conventional designs of cylindrical rotary motors and LOAs are laminated axially and radially, respectively. Radial lamination of the designs of the LOA has the consequences of a small stacking factor which affects in term of reducing air-gap flux density. A new approach of separate formation of stator pole teeth and back iron, in the design of LOA is investigated in [12]. Increasing the stacking factor considerably raises the air gap flux density, which further increases the thrust force density and back electromotive force. In contrast to tubular topology, rectangular topology has superiority on account of simple structure, easy fabrication, and low cost. Stator cores with rectangular-structure are easy to laminate. The most significant elements of the moving magnet LOA, in terms of cost, are the PMs. Rectangular-shaped LOA PMs structures are also rectangular that are low-cost and avoids the complexity that exists in tubular radial magnetized PM. Also, rectangular-shaped PMs have the flexibility to attach numerous small-dimensional PMs to achieve the required PM dimensions. The rectangular LA's stator coils are exposed to the air, lowering the risk of overheating and making it simple to replace defective parts [13].

Meeting the different design output requirements of LOA requires optimization of the design. Determining the dimensions of design parameters and accomplishing the best possible solution within a constrained design space are the goals of achieving optimum design [14]. EM force, which is the important parameter of the LOA, is optimized in [15] by using the finite parametric sweep method. The operating resonance frequency is also influenced by the mass of the mover and is optimized in [15] by selecting the optimum split ratio

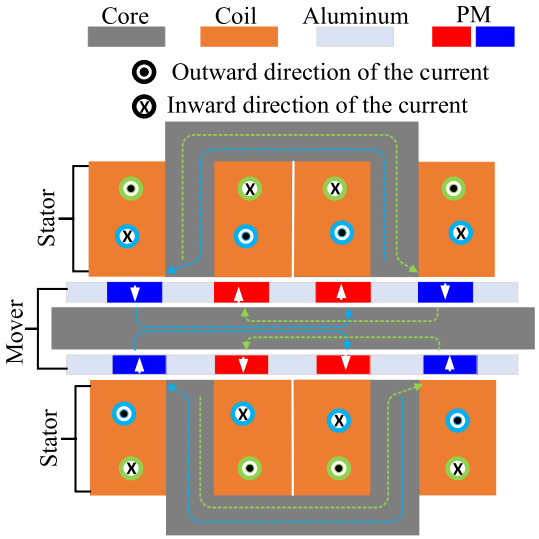

FIGURE 1. 2-D schematic of the investigated LOA.

by utilizing the parametric sweep tool. Detent force which is contrary to EM force is a basic limitation of LOA and is reduced by optimizing the teeth inserted in the axillary stator core placed inside the tubular mover [16]. LOA can be used for different applications like compressors, bio-medical applications, robots, and electric hammers [17].

This paper evaluates the performance of a new design of LOA (rectangular-shaped) for the compressor in portable pumps. A 2-D model is presented, and an explanation of the operating principle is provided. To demonstrate the actual design, a CAD model is presented. All the design parameters are optimized using a parametric finite sweep tool. Output parameters like stroke and EM forces are presented to provide the significance of the investigated LOA topology. It is shown how resonance phenomena influence stroke-to-current ratio, input current, input and output powers, and efficiency depending on the operating input loading frequency. To demonstrate the superiority of the examined LOA, the investigated topology of LOA is evaluated and compared with already built designs of LAs.

II. TOPOLOGY DESCRIPTION AND OPERATING PRINCIPLE

Investigated design topology of the LOA is illustrated in figure 1, which consist of a mover and two stators. Stator, the static part of the LOA, consists of C- shape ferromagnetic core materials and two coils wound across the side legs of the C-shaped core part. Mover, the dynamic part of the LOA is composed of PMs, which are magnetized alternatively radially. Mover back iron provides the least reluctance route to magnetic flux and flows from one stator pole to the corresponding another pole. The gaps between the PMs are filled by using less dense material (aluminum) to build the LOA with the least mover mass and more mechanical strength. Pole faces are enlarged by using pole shoes attached to both sides

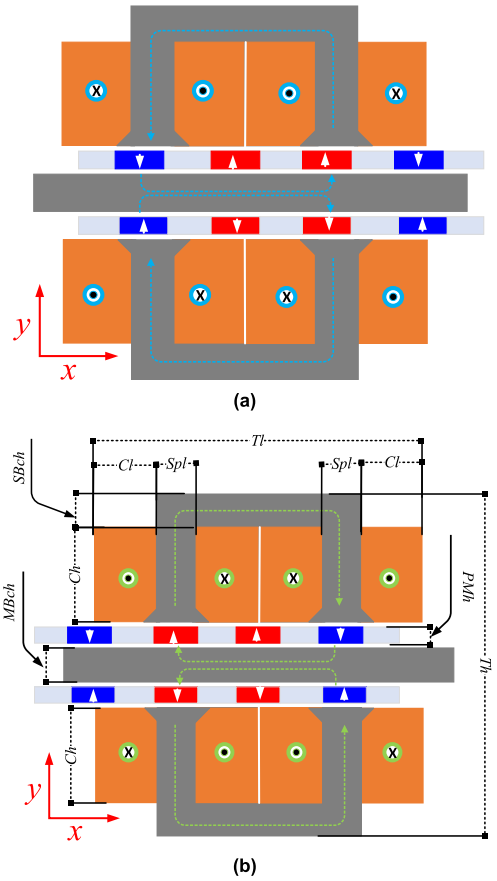

FIGURE 2. 2-D schematic of the investigated LOA at their final mover positions (a) $+x$ final position (b) x final position.

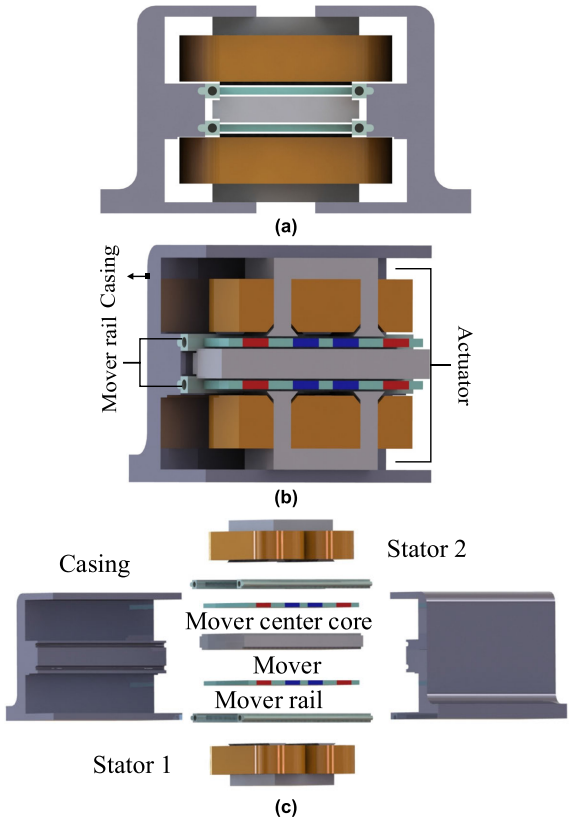

FIGURE 3. 3-D schematic of the investigated LOA (a) front view (b) section view (c) Exploded view.

TABLE 1. Parameter dimensions of the investigated LOA.

Parameter name	SYMBOL	Base value (mm)	Optimized value (mm)
LOA total length	Tl	100	100
LOA total height	Th	100	100
LOA depth	D	120	120
PM height	PMh	4	4
PM length	PMl	15	15
Coil height	Ch	27	29
Coil length	Cl	20	20
Stator back core height	$SBch$	10	8
Mover back core height	$MBch$	10	14
Stator pol length	Spl	10	10
Air gap	Ag	1	1

of the stator poles. Pole shoe helps during the linkage of flux between stator poles and PMs placed in the mover.

Investigated LOA work is based on the phenomenon known as magnetic field alignment, which states that PMs move to the position at which magnetic flux lines encounter the minimum reluctance. Stator coils of the LOA are magnetized in alternate directions, and magnetic flux lines originate from one stator pole and enter the corresponding another stator pole. The simultaneous direction of the magnetic flux density through the lower and upper stator cores are opposite. Due to the opposite directions of magnetic flux lines through the stator's core, the mover receives a uni-directional EM force. When the coils are loaded with the current, having direction shown by symbols, the corresponding direction of magnetic flux density is depicted by arrows, as shown in figure 1. For the current direction, represented by cyan color, the mover receives an EM force toward the $+x$ direction and shifts to $+x$ extreme position, as shown in figure 2(a). By altering the direction of the current (shown by the green color), an EM force is exerted on the mover in a reversed direction, towards the $-x$ axis and displaces the mover to the x final position, as depicted in figure 2(b). Examined LOA uses single-phase AC power to operate; for half cycle of the input loading, the mover shifts to one extreme position and the mover moves to the other extreme position during the remaining half cycle. Initial and optimized dimensions of the parameters of the LOA are presented in table 1. To demonstrate the real view of the investigated design, the CAD model is presented in figure 3 where figure 3(a) shows a compact side view and figure 3(b) illustrates the section view. Section view reveals all parts of the LOA, included in the compact structure. Figure 3(c) depicts the 3-D structures of each part included in the assembly of the LOA. Dimensions

of the parameters are symbolically labelled and shown in figure 2(b).

III. OPTIMIZATION

This section discusses the optimization procedure of investigated design of the actuator. Optimization of the dimensions of different parameters is accomplished by utilizing a finite parametric sweep facility in COMSOL Multiphysics software. The primary aim of the optimization is to provide ease to magnetic flux flow and to design the core part with optimum dimensions. Parameters concerning magnetic field generation were also focused on, and optimum values were considered on the bases of the EM force experienced by the mover. PM position relative to the stator pole is also investigated, and its effect on peak EM force at a mover mean position and average EM force through the overall amplitude of the oscillation (stroke) are analyzed.

Mover back core height (M_{bch}) is optimized while keeping the overall height (T_h) of the actuator constant. Through the parametric sweep method, the dimension of the MB_{ch} is varied, and through specified conditions, the stator core height (S_{ch}) is adjusted by using a relation in the parameters definition portion. During this optimization approach, a specified condition is defined for the stator core height in the parameters dimension portion, which is

$$S_{ch} = \left(T_h - MB_{ch} - 4\times A_g - 2\times PM_h\right)/2 \tag{1}$$

$$C_{nt} = \left(\frac{C_h \times C_l}{W_d^2} - \frac{1}{2}\frac{P_{sh}^2}{W_d^2}\right) C_{ff} \tag{2}$$

In (1), S_{ch} is the stator core height, T_h is the total height of the actuator, MB_{ch} is the mover back core height, A_g is the air gap, and PM_h is the PM height. During this analysis, the coil number of turns are kept updated by using relation (2). In (2), C_{nt} is the coil number of turns, C_h is the value of the coil height, C_l is the value of coil length, W_d is the diameter of the single turn, P_{sh} is the pole shoe length, and C_{ff} is the value of the coil filling factor. Values of the constants are listed in table 1. During mover back core height ($MBch$) optimization, the value of the coil height is also updated by using the relation $C_h = S_{ch} - 10\,[mm]$. This relation demonstrates that the value of back core height is fixed using its dimension of value $10mm$. Figure 4 demonstrates that the mover back core height optimum value is $14mm$ where the dimension of the stator core height is $37mm$.

Total length of the actuator is remained fixed, and the coil length and stator pole length are optimized by using the relation in the parameters dimension portion

$$S_{pl} = (T_l - 4\times C_l)/2 \tag{3}$$

In (3), S_{pl} is the stator pole length, T_l is the overall actuator length, C_l is the coil length. During this optimization process, the value of the C_l changes; hence, the coil turns number is kept varying using (2). Form figure 5, the optimum values of the coil length and stator pole length are $20mm$ and $10mm$, respectively.

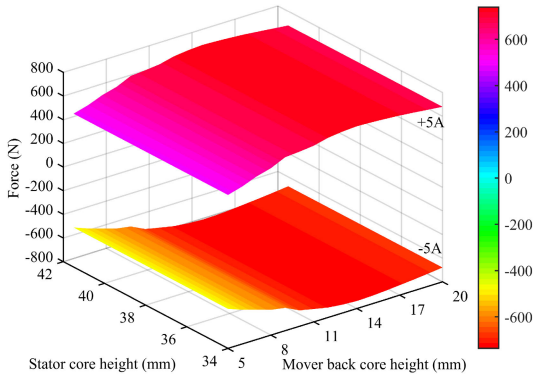

FIGURE 4. Mover back core height optimization.

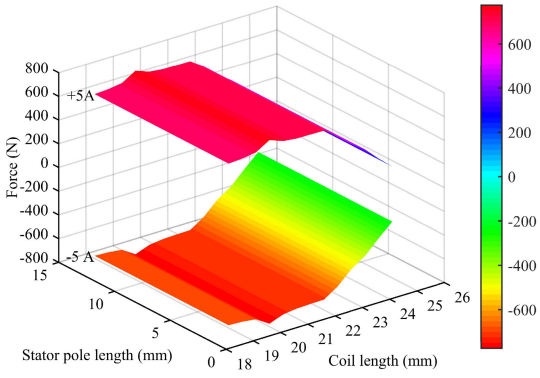

FIGURE 5. Coil length optimization.

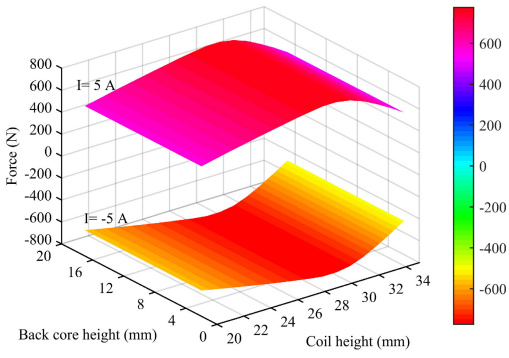

FIGURE 6. Coil height optimization.

Coil height C_h and stator back core height SB_{ch} are optimized by using the relation

$$SB_{ch} = S_{ch} - C_h \tag{4}$$

In (4), the value of the C_h is kept varying, which further changes the value of the SB_{ch}. In this investigation, the number of turns are kept updated by using (2). From the figure 6 it is evident that the optimum value of the C_h is 29 mm where SB_{ch} value is 8 mm.

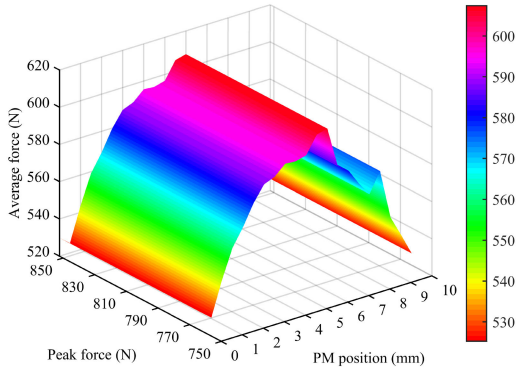

FIGURE 7. PM position optimization for EM force toward +x axis.

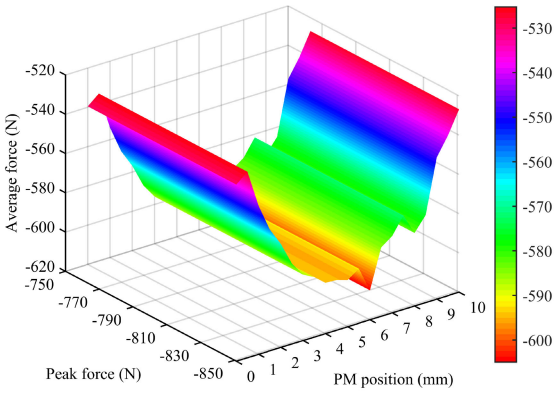

FIGURE 8. PM position optimization for EM force toward −x axis.

PM position relative to the stator pole is also optimized in terms of peak EM force at the mean position of the mover and average EM force through the overall stroke range. PM's initial position was fixed at the mid of the stator pole and displaced along the x-axis. Figure 7 demonstrates the peak and average EM force toward +x-axis, and its optimum value is at $+6mm$ from the initial reference point. Similarly, EM force toward the –x-axis is presented in figure 8. Figure 8 also shows that optimum peak and average EM force values are at $+6mm$ from the initial reference point.

IV. RESULTS AND DISCUSSION

The proposed actuator is simulated using COMSOL Multi-physics FEM software. The coils of the actuator are excited by applying Direct Current (DC) and Alternating Current (AC). Adjacent coils of both upper and lower stators are magnetized by using DC with opposite directions to provide uni-directional Magnetic Flux Density (MFD) in the core of the stator. Similarly, coils of the stator placed at the opposite side of the mover are excited by DC with a reversed direction that produces MFD in the opposite direction in the stator core, and as a result, MFD through the mover back core becomes parallel. This combination of the coil current directions provides uni-directional EM force on the mover of the actuator. By reversing the DC direction through both coils of the stator,

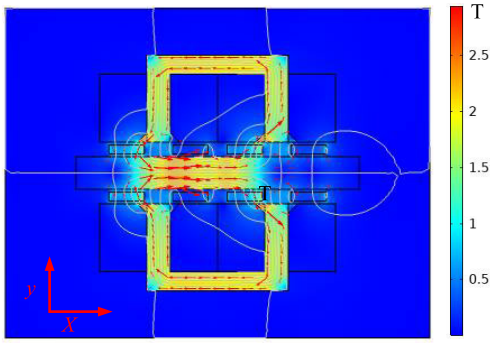

FIGURE 9. Simulated view when mover receive an EM force toward +x axis.

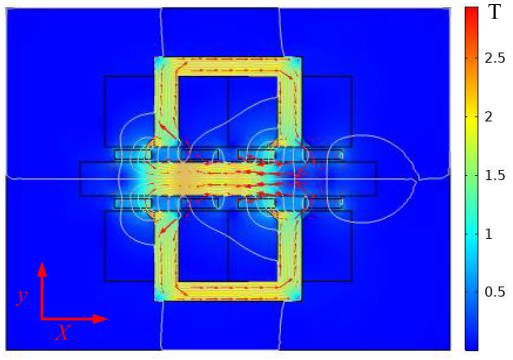

FIGURE 10. Simulated view when mover receive an EM force toward -x axis.

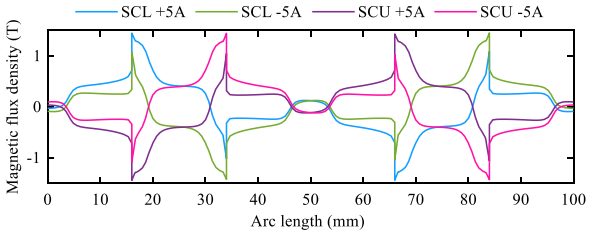

FIGURE 11. MFD linking with stator poles.

the MFD direction becomes opposite, and hence the direction of EM force becomes opposite. Since the suggested actuator design uses a single-phase AC, an EM force is exerted on the mover in the forward direction for the AC half cycle of the AC and an EM force in the backward direction for the remaining half cycle of the AC.

EM force of the LOA is generated due to basic phenomena of the MFD, which states that MFD tends to follow the least reluctance route and mover shifts its position to provide the least reluctance path. Coils current direction combination produces MFD in an anti-clockwise direction in the upper stator core and clockwise in the lower, as depicted in figure 2(a); its simulated view is shown in figure 9. This combination of current directions of both stator coils produce EM force on the mover toward the +x axis to provide the least reluctance path to MFD. Additionally, figure 8 shows MFD at different

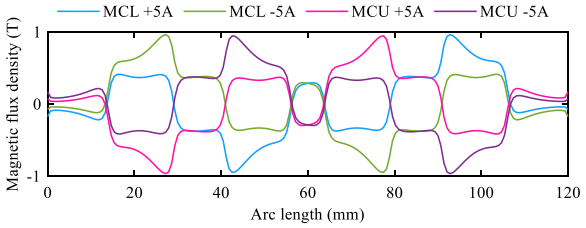

FIGURE 12. MFD linking with mover back core.

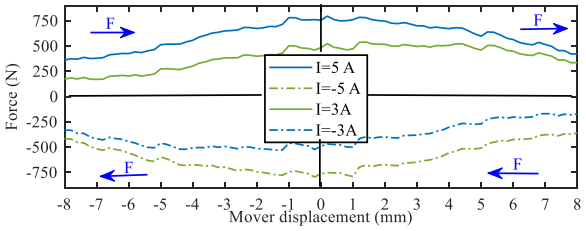

FIGURE 14. EM force at various mover positions.

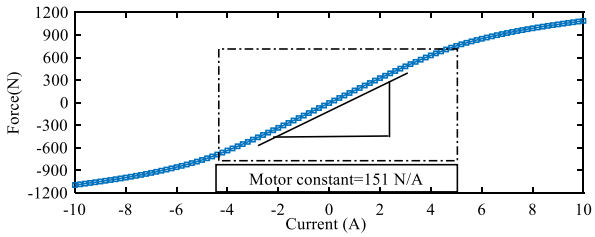

FIGURE 13. EM force for various magnitudes of DC.

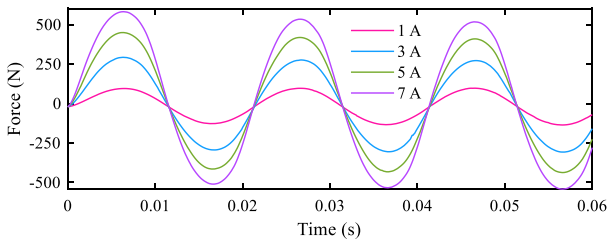

FIGURE 15. Time dependent EM force for various amplitudes of an AC.

portions of the actuator, and its magnitude is shown by using a legend. The direction of the MFD flow is presented by using red arrows. Similar to the figure 2(b), for opposite direction coils current, a simulated view of the actuator is depicted in figure 10. This combination of the coil's current direction provides the EM force toward the –x-axis to provide the least reluctance path to MFD.

Mover of the investigated actuator topology consists of only PMs with the specified direction of magnetization, as discussed in section II. MFD linking between stator poles and mover is measured and depicted in figure 11. During this investigation, coils of the actuator were excited using 5*A* DC and the mover was placed at the mean position. MFD is examined using both DC directions using positive and negative symbols in the legends of figure 11. This figure presents MFD linking with Stator core lower (SCL) and stator core upper (SCU).

The mover back core is housed between two mover portions and provides a returned path to the MFD. There is also a linkage of MFD between the mover and the mover back core. This linkage of MFD is measured and shown in figure 12. Similar to the investigation performed in figure 11, this analysis is accomplished along the mover core lower (MCL) and mover core upper (MCU) parts. Also, for both directions of DC, MFD is measured and presented.

EM force is analyzed towards both directions of the EM force for the different magnitudes of DC and presented in figure 13. Both directions of the DC are used to investigate forward and backward EM forces. Motor constant (MC) which is the averaged EM force per ampere, is calculated by measuring the slope of the EM force curve. MC of the proposed design is $151N/A$, which is measure up to the 5*A* value of the DC because the proposed actuator is optimized by using the 5*A* value of the DC. Furthermore, figure 13 reveals that the proposed design of the actuator provides an identical EM force response toward both directions, which is an indication of the bidirectional nature of the EM force.

EM force at different positions of the oscillating region is measured and shown in figure 14. The positive value of the DC provides a positive EM force, indicating that the mover receives an EM in the forward direction. From figure 14, it is also clear that for a negative value of the DC, the mover receives an EM force in reversed direction. EM force associated with the 2nd and 1st quadrants of figure 14 displaces the mover of the actuator from the negative peak position of the oscillating region to the positive extreme position of the oscillating region. Similarly, EM force having a negative value displaces the mover from the positive final position of the oscillating region to the negative peak position of the oscillating region, as depicted in the 4th and 3rd quadrants of figure 14. This investigation shows that the examined actuator receives significant EM force up to a displacement of value 8*mm* forward and 8*mm*backward. Therefore, the overall displacement region commonly named stroke of the actuator is 16*mm*.

The EM force oscillating nature of the proposed actuator is also analyzed by using time-dependent input loading (AC) to the coils of the proposed actuator, and the EM force response is presented in figure 15. Various amplitudes of the input AC are applied and an EM force response is presented, which shows the oscillating nature of the EM force. Furthermore, by increasing the input AC amplitude, the oscillating EM force amplitude is also improved, which shows variability in the value of EM force.

V. RESONANCE

Traditionally, crankshafts were employed to transform the revolving motion of rotary motors into linear oscillation. In comparison to the traditional actuation approach, the performance of the LOA is significantly enhanced when it

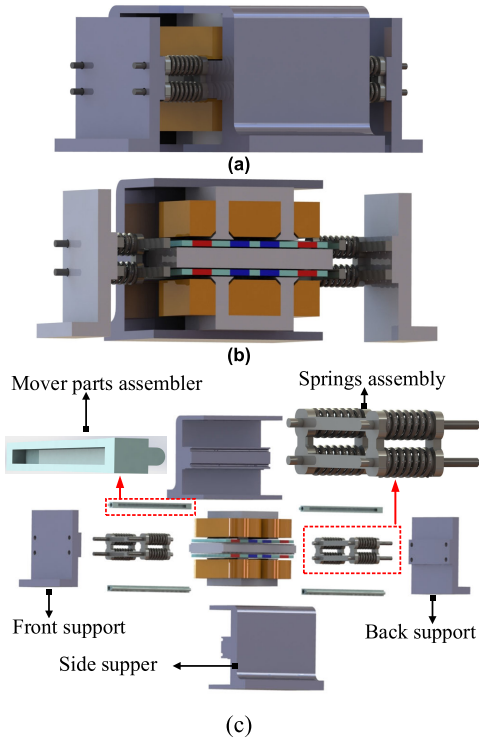

FIGURE 16. Complete setup of the investigated actuator (a) full compact view (b) section view (c) unpacked exploded view.

operates under resonance conditions [2], [3]. When resonance operation is used, it is possible to achieve a feasible output while using a minimum amount of input current. Due to minimal current, the EM force of the LOA becomes smaller, whereas the stroke of the LOA becomes maximum at resonance condition. The LOA's resonance frequency operation has the greatest effect on the ratio of the stroke to current and stroke to EM force [4]. On account of a smaller input current, the efficiency of the system becomes maximum [8]. Moreover, the thermal management of the LOA is also enhanced on account of minimal current flow. The complete mechanical design of the investigated LOA is shown in figure 16, where figure 16 (a) shows a compact view, figure 16 (b) depicts a section view and figure 16 (c) presents a 3-D view of each part of the assembly. In The LOA, two types of resonance can be achieved: one is mechanical resonance and the second one is electrical resonance.

A. MECHANICAL RESONANCE

Mechanical resonance can be achieved by exciting the coils using the frequency of the input loading equal to the mechanical resonance frequency of the actuator. The condition of the mechanical resonance is

$$r_m = \omega_{m(res)}/\omega \tag{5}$$

In (5), $\omega_{m(res)}$ is the mechanical resonance frequency in rad/sec and ω is the frequency of the input electrical loading. When the r_m value becomes unity, mechanical resonance

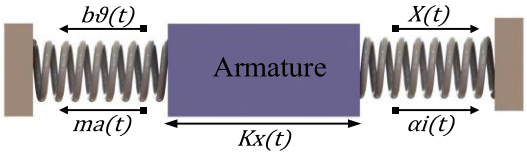

FIGURE 17. Mechanical model of the investigated LOA.

occurs. The mechanical resonance frequency is calculated by using the relation

$$\omega_{m(res)} = \sqrt{k}/m \tag{6}$$

In (6), k is spring stiffness and m is the mover mass. Different types of forces acting on the mover are presented in figure 17. Forces acting on the mover of the actuator, depicted in the mechanical model of the actuator, shown in figure 17 is

$$F_{electromagnetic} = F_{inertial} + F_{damped} + F_{spring} \tag{7}$$

Mathematical expressions for each force associated with the mover as presented in (7) are

$$\alpha i\,(t) = ma(t) + b\vartheta\,(t) + Kx(t) \tag{8}$$

In (8), α is the motor constant, $i\,(t)$ is the time-dependent current,m is the mover mass, $a(t)$ is the acceleration, b is the damping coefficient, $\vartheta\,(t)$ is the mover velocity, K is the spring stiffness and $x(t)$ is the mover displacement.

B. ELECTRICAL RESONANCE

Electrical resonance is achieved by exciting the coil with alternating loading having a frequency equal to the electrical resonance frequency. At electrical resonance conditions, capacitive reactance minimizes inductive reactance, and the circuit becomes resistive [6]. Power loss due to both reactance becomes minimum and the efficiency of the system becomes significantly high. The condition for electrical resonance is

$$r_e = \omega_{e(res)}/\omega \tag{9}$$

In (9), $\omega_{e(res)}$ is the electrical resonance frequency and ω is the frequency of the input electrical loading. At the electrical resonance state, the value of r_e reaches unity. The electrical resonance frequency is calculated by using the relation

$$\omega_{e(res)} = 1/\sqrt{LC} \tag{10}$$

In (10), L is the inductance of the coil and C is the capacitance of the capacitors, attached for creating electrical resonance. The value of the required capacitance is calculated by using the relation

$$C = 1/\omega^2_{e(res)}L \tag{11}$$

The overall electrical circuit model, shown in figure 18, its mathematical representation using Kirchhoff law, is

$$V_{exc(t)} = \mathrm{e}Ri\,(t) + Ldi/dt + 1/C\int i\,(t)\,d\,(t) + v_{bemf} \tag{12}$$

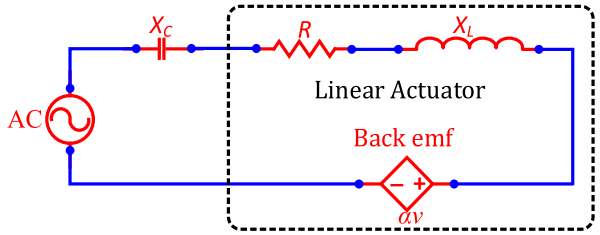

FIGURE 18. Electrical circuit model of the investigated LOA.

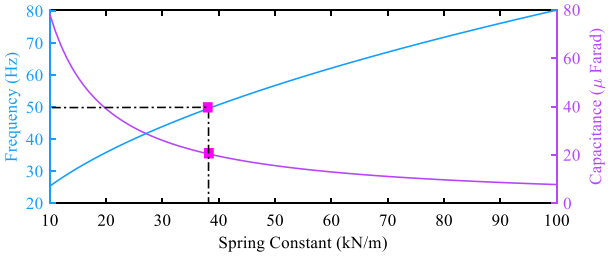

FIGURE 19. Relation of spring constant with mechanical resonance frequency and capacitance.

In (12), $V_{exc(t)}$ is the input voltage, $Ri\,(t)$ is the voltage drop across the resistor, Ldi/dt is the voltage drop due to the inductance of the coil, $1/C\int i\,(t)\,d\,(t)$ is the voltage drop through capacitors and v_{bemf} is the back emf generated due to oscillations of the mover.

C. IMPACT OF RESONANCE ON THE PERFORMANCE OF THE ACTUATOR

Analysis of the different output parameters using basic resonance conditions is presented in this section. Current flowing through the actuator electrical circuit is due to the difference of voltages, which is the difference between applied voltage and back emf. The mechanical resonance frequency is calculated using (6) and presented in figure 19. Moreover, the value of the required capacitance is calculated using equation (11), and its value for different values of the spring constant is shown in figure 19. To design the LOA with a resonance frequency of value $50Hz$, the required spring constant and capacitance are $39kN/m$ and $20\mu F$, respectively.

The voltage difference between applied voltage and back emf is the primary cause of current flow. Due to the smaller value of voltage difference, minimum current is flowing which enhances the efficiency of the design. Relation for calculating voltage difference is derived in terms of the mechanical and electrical parameters using equations (8) and (12), which is

$$\left|V_{diff}\right| = \frac{\vartheta}{\alpha}\sqrt{b^2R^2 + m^2\omega^2\delta_m^2 Z_e + L^2\omega^2\delta_e^2 Z_m} \tag{13}$$

where

$$\left\{\begin{array}{c} \delta_m = 1 - r_m^2 \\ \delta_e = 1 - r_e^2 \\ Z_m = b^2 + m^2\omega^2\delta_m^2/2 \\ Z_e = R^2 + L^2\omega^2\delta_e^2/2 \end{array}\right\}$$

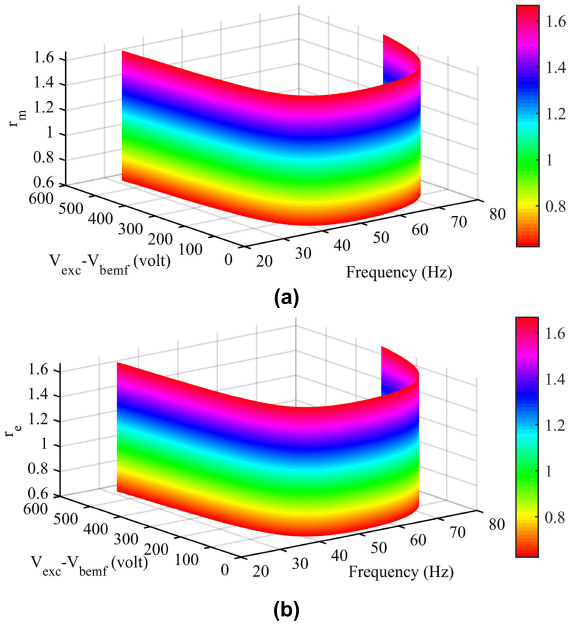

FIGURE 20. Investigation of voltage difference for different values of frequency and resonance conditions (a) Mechanical resonance condition r_m (b) electrical resonance condition r_e.

In (13), δ_m is the mechanical resonance-dependent parameter, δ_e is the electrical resonance-dependent parameter, Z_m is the mechanical impedance and Z_e is the electrical impedance. By putting the values of the constants, equation (13) is simulated for different values of the frequency as shown in figure 20. Figure 20(a) demonstrates the influence of the frequency on the voltage difference ($V_{exc} - V_{bemf}$) and also on the mechanical resonance condition r_m. Similarly, the effect of input electrical loading frequency on the voltage difference and electrical resonance condition r_e are presented in figure 20 (b). Figure 20 reveals that at the resonance frequency, there is the minimum voltage difference between excitation voltage and back emf.

As discussed in the previous paragraph, at the resonance frequency, the difference between applied voltage and back emf results in a small value; hence the current flowing across the coils of the LOA is also minimum. The relation of the current across the LOA circuit is derived using two basic equations (8) and (12), which is

$$|I| = \frac{|V|\,\omega^2}{\sqrt{\Upsilon^2 + \Psi^2}}\sqrt{b^2 + \zeta_m^2} \tag{14}$$

where

$$\left\{\begin{array}{c} \Upsilon = mL\omega^2\left(1 - r_e^2\right)\left(1 - r_m^2\right) - \omega^2(bR + \alpha^2) \\ \Psi = -mR\omega^3\left(1 - r_m^2\right) - bL\omega^3(1 - r_e^2) \\ \zeta_m = \omega m(1 - r_m^2) \end{array}\right\}$$

Equation (14) is simulated to investigate the current across the LOA coil for distinct values of the frequency, as depicted in figure 21. Figure 21 also presents EM force performance for different frequencies of the input loading by using relation $f_m = I\alpha$. Figure 21 reveals that operating the LOA using

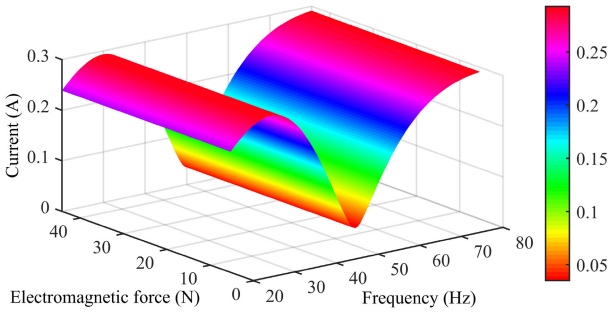

FIGURE 21. Influence of electrical loading frequency on Electromagnetic (EM) force and current.

resonance frequency of the input alternating electrical loading contributes significantly in terms of current.

Stoke is another parameter of the LOA which plays a key role in mass flow rate and output power. By increasing the value of the stroke, the mass flow rate and output power of the LOA increases. Stroke to the current ratio of the LOA is determined by using the relation

$$x/I = \alpha/(\omega\sqrt{b^2 + \zeta_m^2}) \tag{15}$$

In (15), the term mechanical parameter ζ_m gives minimum value at resonance frequency because the value of r_m becomes unity at resonance condition. Similarly, equation (15) can be represented in terms of electrical parameters by replacing $\zeta_m = \zeta_e = \omega m(1-r_e^2)$. Figure 22 demonstrates the impact of frequency on stroke to current ratio, which gives a maximum value at the resonance frequency. Figure 22(a) investigates stroke to the current ratio in the presence of mechanical resonance condition r_m. Similarly, figure 22(b) investigates stroke to current ratio and electrical resonance condition r_e. Figure 22 concludes that resonance frequency operation contributes significantly in terms of the ratio of the stroke to the current.

Velocity of the mover is also an important parameter which is determined by using basic relations of the resonance. The relation of velocity is

$$|\vartheta| = |V|\,\alpha\omega^2/\sqrt{\Upsilon^2 + \Psi^2} \tag{16}$$

Input and output powers and efficiency of the investigated design of LOA are analyzed for distinct values of the input electrical loading frequency, as shown in figure 23. The input power of the LOA is calculated by using the multiplication of input voltage and current. Output power is determined by using the product of EM force and velocity of the mover. The velocity of the mover is calculated using equation (16). Figure 23 shows how the variation between input and output powers gradually reduces as resonance frequency approaches, reaching its efficiency to peak value.

VI. COMPARISON WITH CURRENT DESIGNS OF ACTUATOR

This section compares the suggested design of the LOA with the traditional design of Linear Actuators (LAs) in terms

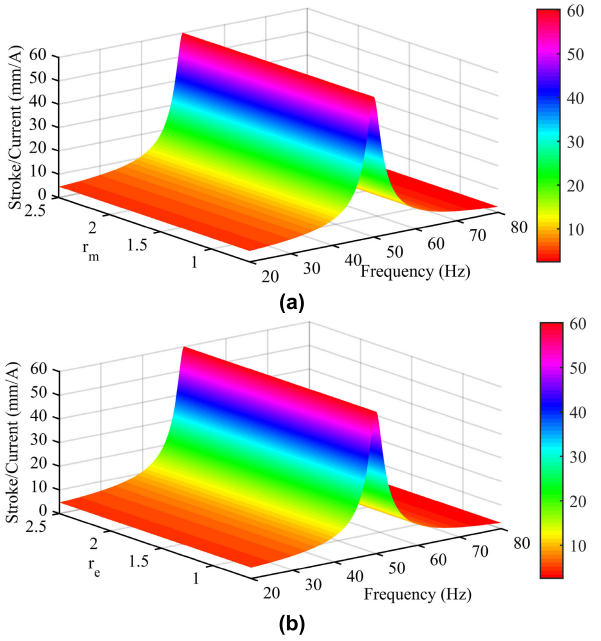

FIGURE 22. Influence of electrical loading frequency on stroke to current ratio of the LOA (a) in term of mechanical resonance condition r_m (b) in term of electrical resonance condition r_e.

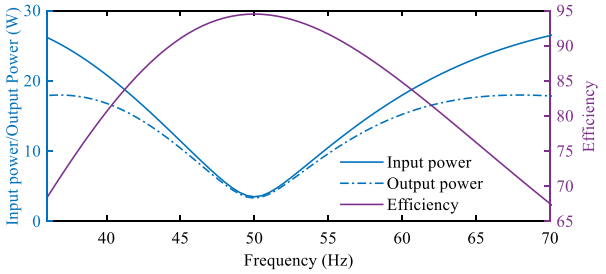

FIGURE 23. Influence of electrical loading frequency on input and output powers and efficiency of the LOA.

of output response and mechanical design parameters. The proposed actuator design is compared with Moving Magnet (MM) LAs to provide a precise comparison. Output performance parameters like stroke and MC are presented. MC per PM mass; EM force per ampere per PM mass of the researched topology, and already built designs of Linear Actuator (LA) designs are compared. Additionally, MC density; EM force per ampere per overall volume of the actuator are also contrasted to provide in-depth information that elaborates the design key aspects.

Key parameters of the examined LOA and also state-of-the-art designs of the LAs are presented in table 3. The stroke of the investigated LOA is 16 mm, which is comparatively greater than the other design tabulated in table 3. MC of the examined LOA is $151N/Amp$, which is more than the other design listed in table 3 except for the design investigated in [2]. The reason for the reduced MC of the proposed design comparatively to [2] is the higher volume of PM utilization in [2]. MC per PM Mass $(N/Kg.Amp)$ of the investigated LOA is higher than that of all designs mentioned in table 3.

TABLE 2. Mechanical, electrical and performance parameter of the design.

Mechanical Parameters		
Parameters name	symbol	value
Mover mass	m	0.392 kg
Spring stiffness	k	39 kN/m
Damping coefficient	b	8 Ns/m
Electrical Parameters		
Parameters name	symbol	value
Resistance of the coil	R	8 Ω
Inductance of the coil	L	$300mH$
Capacitance	C	20 μF
Performance parameter		
Parameters name	symbol	value
Motor constant	α	151 N/Amp

TABLE 3. Topology and performance outcome of the examined and already built designs of LA.

Con-LA	Topology	Stroke (mm)	MC (N/A)	MC per PM mass ($N/Kg.A$)	MC density ($N/mm^3.A$)
[2]	Tubular	12	200	263.744	2.954×10^{-4}
[4]	Tubular	8.8	38	146.957	1.948×10^{-5}
[8]	Tubular	10	48	147.7610	6.23×10^{-5}
[5]	Rectangular	12	120	312.5	1.016×10^{-4}
[13]	Tubular	14	56.6	254.799	2.08×10^{-4}
Proposed	Rectangular	16	151	524.3	1.258×10^{-4}

Similarly, the MC density $\left(\mathrm{N}/\mathrm{mm}^3.\mathrm{Amp}\right)$ of the proposed design is also greater as compared to the designs mentioned in table 3. This investigation has found that the proposed LOA has a strong EM force while utilizing less PM volume and also having a lesser overall volume of the design of the LOA.

The proposed design of the actuator is simple in structure and low-cost on account of utilizing rectangular-shaped PMs and core. By using numerous small dimensional PMs, rectangular PMs are easy to construct and convenient for obtaining desired proportions. The most difficult aspect of tubular LA is creating the lamination to reduce eddy current losses. The core parts of the proposed LOA are rectangular shapes that make it convenient to assemble the laminations. Furthermore, the suggested LOA has an open-structure that improves temperature regulation and the replacement of defective parts.

VII. CONCLUSION

This paper investigates a moving magnet rectangular-shaped LOA of compressor application. The primary objective of the paper is to investigate an alternative topology of tubular-shaped LOA where the lamination of the core material is easy to accomplish. Design topology is explained and its operating principles are elaborated briefly. For better visualization, different views of the CAD model are presented. Dimensions of different parameters that significantly influence the actuator's EM force are optimized with the help of the finite parametric sweep method. PM's position on the mover is optimized to improve the stroke of the investigated LOA. Output parameters like static and dynamic EM force are presented for different input current values. Additionally, the LOA's stroke is investigated for distinct DC magnitudes and for both directions of the DC. The explanation of resonance phenomena and an investigation of its effects on input current, EM force, stroke-to-current ratio, and efficiency are illustrated. The proposed LOA's design parameters and output parameters are compared with those of the most recent LA designs. Proposed LOA design gives superior results regarding motor constant per PM mass and motor constant per overall volume of the design structure. This design of LOA provides significant results while having a simple structure, inexpensive and easy to fabricate.

ACKNOWLEDGMENT

This research work was funded by Institutional Fund Projects under grant no. (IFPIP: 894-135-1443). The authors gratefully acknowledge the technical and financial support provided by the Ministry of Education and King Abdulaziz University, DSR, Jeddah, Saudi Arabia.

REFERENCES

[1] S. Khalid, F. Khan, Z. Ahmad, and B. Ullah, "Design and analysis of modular C-core moving magnet linear oscillating actuator for miniature compressor application," in *Proc. Joint MMM-Intermag Conf. (INTERMAG)*, New Orleans, LA, USA, Jan. 2022, pp. 1–5.

[2] Z. Ahmad, A. Hassan, F. Khan, N. Ahmad, B. Khan, and J.-S. Ro, "Analysis and design of a novel outer mover moving magnet linear oscillating actuator for a refrigeration system," *IEEE Access*, vol. 9, pp. 121240–121252, 2021.

[3] K. Liang, "A review of linear compressors for refrigeration," *Int. J. Refrig.*, vol. 84, pp. 253–273, Dec. 2017.

[4] A. Hassan, A. Bijanzad, and I. Lazoglu, "Dynamic analysis of a novel moving magnet linear actuator," *IEEE Trans. Ind. Electron.*, vol. 64, no. 5, pp. 3758–3766, May 2017.

[5] C.-W. Kim, G.-H. Jang, K.-H. Shin, S.-S. Jeong, D.-J. You, and J.-Y. Choi, "Electromagnetic design and dynamic characteristics of permanent magnet linear oscillating machines considering instantaneous inductance according to mover position," *IEEE Trans. Appl. Supercond.*, vol. 30, no. 4, pp. 1–5, Jun. 2020.

[6] Z. Ahmad, A. Hassan, F. Khan, and I. Lazoglu, "Design of a high thrust density moving magnet linear actuator with magnetic flux bridge," *IET Electric Power Appl.*, vol. 14, no. 7, pp. 1256–1262, Jul. 2020.

[7] C. Li, H. Zou, J. Cai, Y. Jiang, and C. Guo, "Dynamic behavior analysis of a moving coil oil-free linear compressor in refrigeration system," *Int. J. Refrig.*, vol. 133, pp. 235–246, Jan. 2022.

[8] A. Bijanzad, A. Hassan, and I. Lazoglu, "Analysis of solenoid based linear compressor for household refrigerator," *Int. J. Refrig.*, vol. 74, pp. 116–128, Feb. 2017.

[9] S. Mirić, P. Küttel, A. Tüysüz, and J. W. Kolar, "Design and experimental analysis of a new magnetically levitated tubular linear actuator," *IEEE Trans. Ind. Electron.*, vol. 66, no. 6, pp. 4816–4825, Jun. 2019.

[10] C. Pompermaier, K. F. J. Haddad, A. Zambonetti, M. V. F. Da Luz, and I. Boldea, "Small linear PM oscillatory motor: Magnetic circuit modeling corrected by axisymmetric 2-D FEM and experimental characterization," *IEEE Trans. Ind. Electron.*, vol. 59, no. 3, pp. 1389–1396, Mar. 2012.
[11] P. Immonen, V. Ruuskanen, and J. Pyrhönen, "Moving magnet linear actuator with self-holding functionality," *IET Electr. Syst. Transp.*, vol. 8, no. 3, pp. 182–187, Sep. 2018.
[12] K. H. Kim, H. I. Park, S. S. Jeong, S. M. Jang, and J. Y. Choi, "Comparison of characteristics of permanent-magnet linear oscillating actuator according to laminated method of stator core," *IEEE Trans. Appl. Supercond.*, vol. 26, no. 4, pp. 1–4, Jun. 2016.
[13] M. Jawad, Y. Haitao, Z. Ahmad, and Y. Liu, "Design and analysis of a novel linear oscillating actuator with dual stator rectangular geometry," *Appl. Comput. Electromagn. Soc. J. (ACES)*, vol. 36, pp. 1384–1392, Nov. 2021.
[14] S. W. Baek and S. W. Lee, "Design optimization and experimental verification of permanent magnet synchronous motor used in electric compressors in electric vehicles," *Appl. Sci.*, vol. 10, no. 9, p. 3235, Jan. 2020.
[15] S. Akbar, F. Khan, Z. Ahmad, W. Ullah, B. Ullah, and S. Hussain, "Design and experimental analysis of high electromagnetic force density moving magnet linear actuator with end ferromagnetic poles," *IET Electric Power Appl.*, vol. 16, no. 10, pp. 1158–1168, Oct. 2022.
[16] H. Zhang, L. Jin, H. Yu, Z. Xu, X. Wei, J. Leng, and S. Fang, "Detent force reduction design for the C-Core single-phase permanent magnet linear oscillation actuator," *IEEE Trans. Ind. Appl.*, vol. 59, no. 2, pp. 1577–1587, Mar. 2023, doi: 10.1109/TIA.2022.3225369.
[17] J. Sun, C. Y. Luo, and S. Xu, "Improvement of tubular linear oscillating actuators by using end ferromagnetic pole pieces," *IEEE Trans. Ener. Conver.*, vol. 33, no. 4, pp. 1686–1691, Dec. 2018.

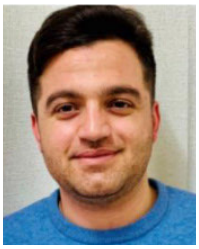

MUHAMMAD JAWAD was born in Pakistan, in 1993. He received the B.S. degree in electrical engineering from the University of Science and Technology Bannu, KP, Pakistan, in 2016, and the master's degree in electrical engineering from Southeast University, Nanjing, Jiangsu, China, in 2021, where he is currently pursuing the Ph.D. degree in electrical engineering. His research interest includes linear permanent magnet motor.

HAITAO YU received the Ph.D. degree from the Huazhong University of Science and Technology (HUST), in 1995. In 1997, he was an Associate Professor with the School of Electric Engineering. From 1998 to 2003, he visits Duke University and Canada for his academic exchange. He is currently a Professor and a Doctoral Supervisor. More than 100 articles have been published, including more than 40 in SCI. His research interests include power electronics, marine power generation, electric vehicles, linear motors, and control research. He is the Director of the China Energy Society. He served as an Editor for the Special Issue on Ocean Power Generation of the *Advances in Mechanical Engineering* (SCI), and a reviewer for various IEEE journals.

ZAHOOR AHMAD was born in KPK, Pakistan, in 1993. He received the M.S. degree in electrical engineering from COMSATS University Islamabad, Abbottabad Campus, Pakistan. He was a Research Exchange Program Member with the GIK Institute for one plus year with the Electrical Machine and Drive Laboratory. His research interests include the design of permanent magnet motors and actuators.

BASHARAT ULLAH (Member, IEEE) received the B.S. degree in electronics engineering from the University of Engineering and Technology, Peshawar, Pakistan, in 2015, the M.S. degree in electrical engineering from the National University of Sciences and Technology, Islamabad, Pakistan, in 2017, and the Ph.D. degree in electrical engineering from COMSATS University Islamabad, Abbottabad Campus, in 2023. Since 2019, he has been a Research Associate with the Research in Design of Electric Machines (RiDEM) Laboratory. His research interests include design, optimization and analysis of rotary and linear hybrid excited flux-switching machines, linear actuators, and polyphase machines and their drives. Furthermore, he is a member of the IEEE-IES Electrical Machines Technical Committee.

BAHEEJ ALGHAMDI received the B.Sc. and M.Sc. degrees in electric power engineering and the Ph.D. degree from the University of Waterloo. He is currently an Assistant Professor with King Abdulaziz University. He joined as a Tenure-Track Assistant Professor with King Abdulaziz University, in 2021, and dedicated to advancing the field through innovative research and teaching. His research interests include control, dynamic analysis, power electronics, and the optimization of microgrids. He is a member of the Smart Grids Research Group.